

AL/EQ-TR-1996-0055

UNITED STATES AIR FORCE
ARMSTRONG LABORATORY



Development of a Technology for In
Situ Remediation of Groundwater

Theodore Mill
Brian Dougherty
Minggong Su
Phillip Cox
David Yao
Stuart Smedley

SRI INTERNATIONAL
333 Ravenswood Avenue
Menlo Park CA 94025-3493

December 1996

19981118 113

Approved for public release; distribution is unlimited.

Envionics Directorate
Environmental Risk
Management Division
139 Barnes Drive, Suite 2
Tyndall Air Force Base FL
32403-5323

DTIC QUALITY INSPECTED 4

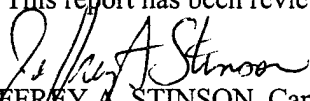
NOTICES


This report was prepared as an account of work sponsored by an agency of the United States Government. Neither the United States Government nor any agency thereof, nor any employees make any warranty, expressed or implied, or assume any legal liability or responsibility for the accuracy, completeness, or usefulness or any privately owned rights. Reference herein to any specific commercial process, or service by trade name, trademark, manufacturer, or otherwise does not necessarily constitute or imply its endorsement, recommendation, or favoring by the United States Government or any agency, contractor, or subcontractor thereof. The views and opinions of the authors expressed herein do not necessarily state or reflect those of the United States Government or any agency, contractor, or subcontractor thereof.

When Government drawings, specifications, or other data are used for any purpose other than in connection with a definitely Government-related procurement, the United States Government incurs no responsibility or any obligations, whatsoever. The fact that the Government may have formulated or in any way supplies the said drawings, specifications, or other data, is not to be regarded by implication, or otherwise in any manner construed, as licensing the holder or any person or corporation; or as conveying any rights or permission to manufacture, use or sell any patented invention that may in any way be related thereto.

This technical report has been reviewed by the Public Affairs Office (PA) and is releasable to the National Technical Information Service, where it will be available to the general public, including foreign nationals.

This report has been reviewed and is approved for publication.


JEFFREY A. STINSON, Capt, USAF, BSC
Project Officer


ALLAN M. WEINER, Lt Col, USAF
Chief, Environmental Risk Management Division

DRAFT SF 298

1. Report Date (dd-mm-yy) December 1996		2. Report Type Final		3. Dates covered (from... to) July 1995 to February 1996	
4. Title & subtitle Development of a Technology for In Situ Remediation of Groundwater				5a. Contract or Grant # F08637-95-C-6032	
				5b. Program Element # 63716D	
6. Author(s) Theodore Mill, Brian Dougherty, Minggong Su, Philip Cox, David Yao, and Stuart Smedley				5c. Project # 4223	
				5d. Task #	
				5e. Work Unit # B76A	
7. Performing Organization Name & Address SRI International 333 Ravenswood Avenue Menlo Park, CA 94025-3493				8. Performing Organization Report #	
9. Sponsoring/Monitoring Agency Name & Address Armstrong Laboratory Environics Directorate Environmental Risk Management Division 139 Barnes Drive, Suite 2 Tyndall Air Force Base, FL 32403-5323				10. Monitor Acronym USAF	
				11. Monitor Report # AL/EQ-TR-1996-0055	
12. Distribution/Availability Statement Approved for public release. Distribution unlimited.					
13. Supplementary Notes					
14. Abstract This report responds to the need of the Air Force to develop new technologies for environmental compliance and site remediation. Effective and efficient treatment of contaminated groundwater is of great importance for Air Force operations, where significant volumes of dilute aqueous waste can be generated and leak into the soil and thence the aquifer. Conventional disposal methods, primarily pump-and-treat, often are impractical or too costly, so that use of aqueous chemical oxidation to treat the contaminants in situ is an attractive alternative for reducing concentrations to acceptable limits.					
15. Subject Terms Cyanoacetophenone, hydrogen peroxide, hydrozyl radical, electrolyte					
Security Classification of			19. Limitation of Abstract	20. # of Pages	21. Responsible Person (Name and Telephone #)
16. Report Unclassified	17. Abstract Unclassified	18. This Page Unclassified	Unlimited	38	Capt Jeffrey A. Stinson (904) 283-6254

PREFACE

This report was prepared by SRI International, 333 Ravenswood Avenue, Menlo Park, California 94025-3493 under contract F0863-7-95-C-6032 for the Department of the Air Force, Armstrong Laboratory, Environics Directorate, Tyndall Air Force Base, Florida.

This report summarizes work done between 28 July, 1995 and 27 February, 1996. Cpt. Jeff Stinson was the Air Force Project Officer.

CONTENTS

SECTION I.....	1
Introduction	1
Objectives	1
Background	2
Scope and Approach.....	3
SECTION II.....	4
Development of Electrochemical Conditions.....	4
SECTION III.....	13
Development and Optimization of Oxidation Catalysts.....	13
Competition Kinetics.....	18
Zero Valent Metal Oxidation Promoters	23
M(0) Promoted Oxidations	29
SECTION IV.....	30
Discussion and Conclusions.....	30
SECTION V.....	32
Experimental Methods	32
CATALYST/PROMOTER EXPERIMENTS	36
REFERENCES.....	38

LIST OF FIGURES

1	Loss of CAP in the presence of $\text{FeO}(\text{OH})$ or Fe_3O_4 with or without added H_2O_2	14
2	Measured loss of cyanoacetophenone (CAP) in the presence of H_2O_2 and Fe-gel at various pH	16
3	CAP decomposition in FeO_x suspension of pH 4, 5 and 6. Each time point represents addition of H_2O_2 to give 180 μM concentration	17
4	ABSA decomposition in pH 4 FeO_x suspension. Each time point represents addition of H_2O_2 to give 180 μM concentration	17
5	Sequential oxidation of ABSA and CAP with FeO_x at pH 4. Each time point represents addition of H_2O_2 to give 180 μM concentration	18
6	Competitive oxidation of CAP and ABSA in pH 2 Fe^{3+} solution with 85 μM aliquots of H_2O_2	19
7	Competition kinetic plot of \ln ABSA versus \ln CAP for pH 2 oxidation	20
8	Competitive oxidation of CAP and ABSA in pH 4 FeO_x suspension with 85 μM aliquots of H_2O_2	21
9	Competition kinetic plot of \ln CAP versus \ln ABSA for pH 4 oxidation	21
10	CAP oxidation using $\text{Fe}(0)$ and FeO_x with H_2O_2 at pH 4	25
11	CAP decomposition with 10 μM $\text{Fe}(0)$ and 200 μM H_2O_2	25
12	CAP oxid with $\text{Fe}(0)$ and 66-200 μM H_2O_2	26
13	CAP oxidation using 0.13 g vs 0.06 g 10 μM Fe, with 0.200 mM H_2O_2	26
14	The effect of pH on the rate of oxidation of CAP with 22 mM 10 μM $\text{Fe}(0)$ and 200 μM H_2O_2	27
15	CAP and H_2O_2 decomposition in flow system with 0.5 g Fe/25 g sand	28
16	CAP oxidation with several metals at pH 4 with 200 μM H_2O_2	29
17	Electrochemical cell use to optimize hydrogen peroxide generation	33
18	Pulse waveform used to generate hydrogen peroxide	34

LIST OF TABLES

1	Values of the baseline operating parameters	5
2	Effect of electrode configuration on the concentration of hydrogen peroxide	7
3	Effect of pulse waveform on the concentration of hydrogen peroxide	8
4	Effect of current magnitude on the rate of generation of hydrogen peroxide.....	9
5	Effect of current magnitude and bed length on the rate of generation of H_2O_2 ..	10
6	Effect of electrolyte salt on the rate of generation of hydrogen peroxide	11
7	Oxidation of CAP and ABSA by hydrogen peroxide with different iron oxide catalysts.....	24
8	Test values of the parameters which define the pulse waveform.....	35

SECTION I

INTRODUCTION

This project responds to the need of the Air Force to develop new technologies for environmental compliance and site remediation. Effective and efficient treatment of contaminated groundwater is of great importance for Air Force operations, where significant volumes of dilute aqueous waste can be generated and leak into the soil and thence the aquifer. Conventional disposal methods, primarily pump-and-treat, often are impractical or too costly, so that use of aqueous chemical oxidation to treat the contaminants *in situ* is an attractive alternative for reducing concentrations to acceptable limits.

Of the current technologies for destruction of trace organic contaminants in water, low temperature chemical oxidation to CO_2 and water is often the preferred method. A number of methods exist for rapid and efficient oxidation of organics in water, which are based on combinations of peroxide, ozone, and/or UV light or ferric ion. These systems are collectively termed advanced oxidation processes or technologies (AOPs or AOTs) and generate hydroxyl radical ($\text{HO}\cdot$) as the effective oxidant for transforming organic compounds into simple acids (formate, acetate or glyoxate) or to CO_2 and water.

We selected the combination of peroxide and metallic iron as the best way to generate $\text{HO}\cdot$ for in situ treatment using a two stage process for (1) generating hydrogen peroxide (H_2O_2) in a contaminated groundwater stream by electrochemically converting water to dilute H_2O_2 in situ and (2) oxidizing trace organic pollutants in the water stream by flowing the H_2O_2 -organic solution through a suitable metallic iron catalyst bed to convert H_2O_2 to hydroxyl radical ($\text{HO}\cdot$) and effect oxidation.

OBJECTIVES

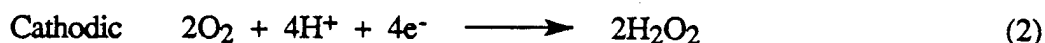
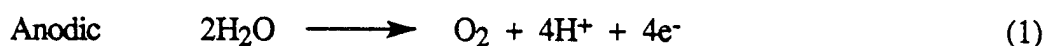
The primary objective of this study is to demonstrate, on a laboratory scale, the effectiveness of an electrochemical oxidation technology for *in situ* destruction of organic groundwater pollutants. The principal elements of our approach are 1) a parametric study of the electrochemical and oxidation factors affecting the efficiency of pollutant oxidation; 2) a long-term

study of reactor activity under simulated *in situ* conditions; and 3) in collaboration with Fluor Daniel, design of a prototype reactor suitable for demonstration at an Air Force site.

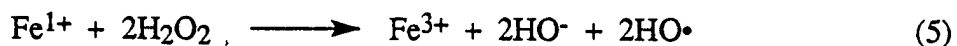
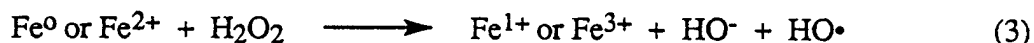
BACKGROUND

Electrochemical Oxidation System

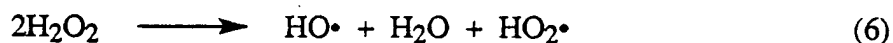
The two-stage oxidation system first converts water to H_2O_2 , using a double pulse potentiostatic technique at the cathode, without the addition of any supporting electrolyte and then converts H_2O_2 to HO radical (HO^\bullet) by reaction with $\text{Fe}^{2/3+}$ or metallic (zero-valent) iron (ZVI) surfaces. The electrochemical reactions to form HP from water are



The reactions to form HO^\bullet from peroxide $\text{Fe}^{2/3+}$ or ZVI are



where $\text{Fe}^{2/3+}$ may be in solution or on the surface of an FeO_x particle. The reaction of $\text{Fe}^{2/3+}$ with H_2O_2 is catalytic in $\text{Fe}^{2/3+}$:



The reaction with Fe^0 is stoichiometric, consuming one Fe^0 for each three HO^\bullet formed.

In practice, the electrode and catalyst systems are electrically separated to minimize H_2O_2 losses or lowering of the current efficiency by unwanted electrochemical cycling of ferric ion. HO^\bullet

is the actual oxidizing agent for organic contaminants in the water. Figure 1 shows the test cell used to evaluate and optimize the electrochemical and catalyst system.

Peroxide Oxidations Catalyzed by FeO_x

We conducted a computerized search of the chemical literature to determine what is known about catalysts for decomposing H_2O_2 and oxidizing organic compounds. The search uncovered about 650 citations extending back to 1965. Only about 150 titles were sufficiently interesting to warrant more detailed examination and all but 10-15 focused only on decomposition of H_2O_2 , without involvement of organics. We found no papers which examined oxidation of organic compounds by H_2O_2 on a heterogeneous metal catalyst, except for the one published in 1989 on oxidations of phthalic and benzoic acids with peroxide and FeO_x catalysts (Mill et al., 1989). That study showed a relationship between sorption of phthalic and benzoic acids on the catalyst and their oxidation: benzoic acid did not sorb or oxidize, whereas phthalic acid sorbed and oxidized

SCOPE AND APPROACH

The study was aimed at developing an integrated laboratory scale electrochemical oxidation reactor which we could use to conduct long term reliability tests on a model groundwater stream. The model stream would contain one or more organic compounds in the ppm range as well as appropriate levels of inorganic ions and dissolved organic matter. The principal elements of our planned approach were (1) a parametric study of the electrochemical and oxidation factors affecting the efficiency of pollutant oxidation; (2) a long-term study of reactor activity under simulated in situ conditions; and (3) in collaboration with Fluor Daniel, design of a prototype reactor suitable for demonstration at an Air Force site.

Initial experiments were conducted to independently optimize the electrochemical system for oxidizing water to H_2O_2 and the catalyzed oxidation of organic compounds with heterogeneous iron catalysts. After the two components were optimized we planned to combine the systems in a single flow unit for additional integration and optimization and long term testing. Much of the optimization testing for the electrochemical system was complete at the time the contract terminated. A new catalyst or promoter, based on metallic iron, was being tested as a superior oxidation promoter and an integrated flow system had been constructed, but not yet tested.

SECTION II.

DEVELOPMENT OF ELECTROCHEMICAL CONDITIONS

The principal objectives of this task were to determine the most efficient electrochemical pulse conditions for the generation of hydrogen peroxide from water at a carbon electrode. Additional objectives were to elucidate the effect of electrode placement, current density, and possible interferences from dissolved species, especially carbonate/bicarbonate and Fe^{2+} , on the efficiency of peroxide generation.

A three-piece electrochemical cell was constructed for the optimization study (see Experimental Methods). The cell was constructed from glass to avoid reactions of peroxide with either plastic or metal. A reactor designed for field use is most likely to be fabricated from plastic, but glass was appropriate for the cell used in the initial work to determine the best pulse type, electrode placement, and to examine the influence of various dissolved species on the rate of peroxide generation.

System Verification and Selection of Baseline Test

An initial experiment was performed to test the cell and to establish an appropriate operating procedure. For this test, a recirculating flow system with a flow rate of 9 mL min^{-1} , was used to concentrate the peroxide in the reservoir. The test solution used in this experiment was 540 mL of distilled, deionized water, with no added supporting electrolyte. The volume of the test solution and the flow rate were such that the entire contents of the reservoir passed through the cell once every hour. The electrochemical pulse regime during this initial test was a 5 mA anodic current pulse for 0.1 s, followed by a 5 mA cathodic current pulse for 0.4s. However, the voltage across the electrodes required to sustain these currents was more than 10 V, beyond the range of the instrument used. Therefore, the solution was acidified to about pH 4 by adding a few drops of concentrated sulfuric acid. After five hours, the peroxide concentration in the solution was measured by uv-vis spectroscopy to be $\approx 65 \mu\text{M}$ (2.2 ppm).

This test confirmed that the cell and test equipment were behaving as expected, and that H_2O_2 could be generated using the double-pulse technique. It also revealed that in the absence of any supporting electrolyte, high cell voltages were required to achieve modest cell currents, a

combination which could lead to high energy costs for a real-world reactor. Although adding a supporting electrolyte is not an option for a field test reactor, it must be recognized that groundwater contains a suite of ions which will function as supporting electrolytes in a real system. Therefore, it was appropriate to add a small amount of supporting electrolyte to the test solutions studied here. Sodium sulfate, Na_2SO_4 , was chosen as supporting electrolyte because Na^+ ions are a common constituent in groundwater and neither Na^+ nor SO_4^{2-} will effect the production or stability of hydroperoxide.

To better mimic the operation of a field reactor, the solution flow through the cell was changed from the recirculating system used in the initial test to a once-through flow system, in which the test solution flowed from the reservoir, through the cell, and the effluent was collected in a second, outlet reservoir. A flow rate of 1 to 2 mL min^{-1} was used. For the cross-sectional area of the cell, 5.1 cm^2 , this equivalent to $\sim 100 \text{ gal ft}^{-2} \text{ day}^{-1}$, about 10 to 100 times faster than a typical aquifer flow rate but the smallest practical at the small bench scale of the present development stage. Testing at slower flow rates required a larger diameter cell and was deferred to the longer term tests planned later. Anodic and cathodic currents of 2 mA were used, with pulse durations of 0.1 s 0.4 s, respectively. Under these conditions, the steady-state peroxide concentration in the solution exiting the cell was $\sim 240 \text{ uM}$ (8.2 ppm). This set of operating parameters, summarized in Table 1, was selected as the baseline.

Table 1. Values of the baseline operating parameters

Parameter	Value
Electrode cross-section	5.1 cm^2
Anode length	1.1 cm
Cathode length	4.4 cm
Flow rate	1 to 2 mL min^{-1}
Supporting electrolyte	1 mM Na_2SO_4
Anodic current magnitude	2mA
Anodic pulse duration	0.1 s
Cathodic current magnitude	2mA
Cathodic pulse duration	0.4 s

Effect of electrode placement

Oxygen is consumed as a reactant during both the electrochemical peroxide generation state of the reactor and in the oxidation reaction between the contaminant molecule and the hydroxyl

radical. This means that the two processes must compete for the available O_2 , so maintaining a high concentration of O_2 is vital to the overall effectiveness of the process.

There are three major sources of O_2 in this system: O_2 dissolved in the solution at the start of the test; O_2 generated at the cathode during the initial anodic pulse; and O_2 generated at the anode during the cathodic pulse. In the small scale laboratory tests described here, no efforts were made to de-oxygenate the test solutions prior to commencing the experiment or to exclude O_2 from the system, since, in any case, O_2 was being generated during the experiment. Consequently, it is reasonable to assume that the test solutions are O_2 -saturated and that the concentration of O_2 dissolved in the test solution is therefore ≈ 1 mM (32 ppm). This may not be the case in a natural aquifer, however, which may have little or no dissolved O_2 .

Oxygen generated at the cathode during the initial anodic pulse is available for both reduction to peroxide and for oxidation of the contaminant. However, O_2 generated at the cathode can only be reduced to H_2O_2 at some point on the cathode surface downstream from the site at which it was generated, assuming that it reacts as dissolved or gaseous O_2 , or, alternatively, at the site at which it was generated assuming that it reacts as adsorbed O_2 . Therefore, this source of O_2 is effectively always "downstream" with respect to both reactor subsystems (electrochemical and catalytic). For the baseline condition of a 2 mA current, assuming Faraday's Law, O_2 is generated at the cathode at the rate of $6.2 \times 10^{-2} \mu\text{mol min}^{-1}$.

The third source, O_2 generated at the anode during the cathodic pulse, can be either upstream of both processes, or downstream of the cathode but upstream of the catalyst. (The third alternative, downstream of both, is not of interest). Under the baseline conditions, oxygen is generated at the anode at the rate of $2.5 \times 10^{-1} \mu\text{mol min}^{-1}$. If the anode is upstream of the cathode, O_2 from this source will be available to both the electrochemical process and the oxidation process. However, if the solution flow rate is low enough and the efficiency of peroxide generation high enough, most of the O_2 present in the system may be converted to peroxide, leaving too little to oxidize the contaminants. On the other hand, if the anode is placed downstream of the cathode, the O_2 generated here will be available to the catalyst, but not to the cathode for conversion to peroxide. This may lead to H_2O_2 concentrations too low to produce sufficient quantities of the hydroxyl radical to completely oxidize any contaminants. Furthermore, peroxide generated at the cathode may be oxidized at the anode if it is downstream of the cathode.

Therefore, the effect of the placement of the anode and cathode with respect to the direction of the solution flow was investigated. These tests were performed without catalyst or contaminant, since our primary objective at this stage of development was simply to see what effect electrode

position had on the concentration of peroxide in the test solution. Three configurations were considered: anode upstream; anode downstream; and sandwiching the cathode between two anodes. In the latter configuration, it was assumed that the two anodes each carried half the current, since they had the same size (1.1 cm thick) and were made of the same material (graphite felt).

The results are summarized in Table 2. In all cases, the tests were performed using the baseline conditions described above and the typical test procedure described in the Experimental Methods Section below. The data are presented both as the rate of production of H_2O_2 , in μmol per minute, and as a concentration, in ppm. The rate of generation of peroxide is the parameter of interest, since it is independent of the solution flow rate; the concentration is not. However, the concentration is the parameter measured experimentally; the peroxide generation rate is calculated by multiplying the concentration ($\mu\text{mol ml}^{-1}$) by the measured flow rate (ml min^{-1}). For the purposes of comparison, the concentrations listed in Table 2 (and all the Tables which follow) are calculated from the tabulated H_2O_2 generation rate, assuming a solution flow rate of 1 mL min^{-1} . The tabulated current efficiency is the percentage of the current passed during the cathodic step required to generate H_2O_2 at the tabulated rate, which is calculated from the charge passed, Faraday's Law, and the solution flow rate through the cell.

Table 2. Effect of electrode configuration on the concentration of hydrogen peroxide.

Electrode Configuration (Upstream \rightarrow Downstream)	H_2O_2 Generation Rate $\mu\text{mol min}^{-1}$	H_2O_2 Concentration ppm	Current Efficiency %
Anode \rightarrow Cathode	0.240	8.2	48
Cathode \rightarrow Anode	0.034	1.7	9
Anode \rightarrow Cathode \rightarrow Anode	0.146	5.6	34

It is clear from Table 2 that the best configuration is to place the anode upstream of the cathode, which gives a H_2O_2 -generation rate of $0.240 \mu\text{mol min}^{-1}$. At a flow rate of 1 mL min^{-1} , this corresponds to a concentration of 8.2 ppm. The current efficiency was 48%. When the anode is positioned downstream from the cathode, H_2O_2 is generated at only 14% of the rate at which it is generated when the anode is upstream from the cathode. When the cathode is sandwiched between two equivalent anodes, the generation rate is halved. These results strongly imply that the primary source of O_2 for the electrochemical generation of H_2O_2 is oxygen generated at the anode during the cathodic pulse. It should be noted that, if all the O_2 generated at the anode is converted to peroxide

at the cathode, the maximum possible current efficiency is 50%, since four electrons are required to generate O_2 from H_2O but only two are required to generate H_2O_2 from O_2 . The balance of the charge at the cathode is used to generate H_2 .

Effect of the Pulse Waveform

Table 3 lists the rate of generation of H_2O_2 at the cathode for the four pulse waveforms tested. The pure DC waveform gives the fastest actual H_2O_2 generation rate, $0.26 \mu\text{mol min}^{-1}$. This is not totally unexpected since in this case H_2O_2 is being generated continuously at the electrode, whereas in the other cases the electrode is anodic (generating oxygen) for part of the time. The anodic pulse does seem to have a beneficial effect from the viewpoint that the current efficiency is improved; otherwise, the amount of H_2O_2 generated would scale linearly with the fraction of the time that a cathodic current is applied to the electrode. The fact that the efficiency is greater than 50% during the symmetrical pulse (0.4s anodic 0.4s cathodic) suggests that relatively more of the O_2 generated at the cathode during the anodic pulse is being converted to peroxide under these conditions.

It also appears that the relative duration of the two pulses is more important than the absolute pulse duration; both the 0.1s/0.4s and 10s/40s anodic/cathodic combinations lead to virtually identical results. This is good from a practical viewpoint since the double layer charging time at very large electrodes (such as would be used in a real reactor) would require longer pulses for the process to be effective. Furthermore, the cost of the electronics required to perform the pulses would be lower if longer pulse times were used.

Table 3. Effect of pulse waveform on the concentration of hydrogen peroxide.

Pulse Duration Anodic — Cathodic	H_2O_2 Generation Rate $\mu\text{mol min}^{-1}$	Concentration ppm	Current Efficiency %
0.1 s — 0.4 s	0.24	8.2	48
0.4 s — 0.4 s	0.18	6.1	56
10 s — 40 s	0.24	8.3	50
0 s — DC	0.26	9.0	40

It is important to note that the current efficiencies listed in Table 3 consider only the amount of charge passed during the cathodic pulse. Charge passed during the anodic pulse is wasted since

no peroxide is generated during this step. If this component of the overall charge passed is considered, the efficiency of the 1:1 pulse is reduced to 28% and that of the 1:4 pulses to 40%. The current efficiency of the DC pulse remains 40%. In other words, although the presence of the anodic pulse apparently improves the current efficiency of the subsequent cathodic pulse, the overall current efficiency is less than or equal to the pure DC case. Since the total (electrical) energy requirements of the system is proportional to the total amount of charge passed, the pure DC pulse is probably the most cost-effective, since it is the simplest to implement. On the basis of these results, the pure DC waveform is probably the best choice for an *in situ* system. Unless indicated otherwise below, the pure DC waveform was used in the remainder of the tests described below.

Effect of Current Density

The effect of current density on the peroxide generation rate is shown in Table 4. The rate of generation of peroxide is higher the higher the current, so that a higher concentration of peroxide is obtained at any given flow rate. However, the current efficiency is lower and the cell operating voltage is higher the higher the current. This means that the energy requirements in terms of kWh per mole of H_2O_2 generated are higher the higher the current. The data in Table 4 also show that the efficiency is affected by the supporting electrolyte, being substantially higher when Na_2CO_3 is used than when Na_2SO_4 is used; this is discussed in more detail below.

Table 4. Effect of current magnitude on the rate of generation of hydrogen peroxide.

Current mA	H_2O_2 Rate $\mu\text{mol min}^{-1}$	Concentration ppm	Current Efficiency %
1 ^a	0.21	7.1	63
2 ^a	0.38	12.9	57
2	0.24	8.2	38
4	0.41	13.9	33

a. 1 mM Na_2CO_3 solutions; remainder are 1 mM Na_2SO_4 solutions.

Since the current efficiency is higher the lower the current, the operating costs in terms of electrical energy will be lower if a lower current is used. However, use of a higher current may reduce the size of a reactor for an underground system, thereby reducing the setup costs. In addition, clean-up time may be shorter at the higher current so that the higher operating costs will

be incurred over a shorter time period. This is particularly so for the case of an aquifer having a high pollutant concentration and/or a fast hydraulic flow rate. Clearly, a trade off between the H_2O_2 generation rate and the current efficiency (hence operating cost) will be required in a full scale system.

Effect of Electrode Bed Length

Table 5 summarizes the H_2O_2 generation rate for two different bed lengths. The cross-sectional area of the cathode bed is the same for both lengths, so the current density expressed on the basis of cross-sectional area is the same for both cathode lengths, for the same current magnitude. However, because the graphite felt cathodes are highly porous, the actual surface area is directly proportional to the cathode volume, and hence length (since the cross-section is the same). This means that the 2.5 cm long cathode has approximately half the surface area of the 5.0 cm long cathode. Accordingly, a current magnitude of 2 mA applied to the shorter cathode is about the same effective current density as a current of 4 mA applied to the longer cathode.

Table 5. Effect of current magnitude and bed length on the rate of generation of H_2O_2 .

Current mA	H_2O_2 Generation Rate $\mu\text{mol min}^{-1}$	H_2O_2 Concentration mM (ppm)
Working electrode: 5.1 cm^2 area; 5.0 cm long.		
1	0.21	0.21 (7.1)
2	0.38	0.38 (12.9)
2 ^a	0.24	0.24 (8.2)
4 ^a	0.41	0.41 (13.9)
Working electrode: 5.1 cm^2 area; 2.5 cm long.		
1	0.28	0.28 (9.5)
2	0.45	0.45 (15.3)

a. 1 mM Na_2SO_4 solutions; remainder are 1 mM Na_2CO_3 solutions.

As described above, higher currents lead to higher H_2O_2 generation rates, although the current efficiency is lower. This is true regardless of the size of the cathode used. Comparing the amount of peroxide generated for 1 mA on the short cathode and 2 mA on the long one, it is apparent that more peroxide is generated when the electrode is longer for the same current density. For the 2 mA/4 mA pair, the H_2O_2 generation rate is about the same regardless of the bed length,

although the use of different supporting electrolytes in this case makes comparison difficult. This probably indicates that for any given current density (expressed on the basis of real surface area) there is an optimum bed length. If the bed is too short, not all the O_2 is reduced to peroxide during the time that it is in contact with the electrode before being swept downstream due to the solution flow. On the other hand, if the electrode bed is too long then at best some parts of its surface are inactive and at worst peroxide may itself be further reduced to OH^- ions.

The relationship between bed length, current density, and solution flow rate, and the rate of generation of peroxide is vital to determining the likely size, operating cost, and clean-up time of a field-scale reactor. The initial tests described here show that higher currents make more H_2O_2 but at a lower efficiency. The effectiveness of the catalyst, concentration of pollutant, and hydraulic flow rate of the aquifer will essentially determine where the balance between current and efficiency must be placed.

Effect of Carbonate and Ferrous Ions

Table 6 shows the effect of carbonate anions and ferrous cations on the rate of generation of H_2O_2 . When carbonate ions are present, the amount of H_2O_2 generated is about 50% more than in the SO_4^{2-} case. It is not immediately clear why this is so, but may be due in part to a higher solution pH in the case of the carbonate (pH ~ 6 for Na_2SO_4 solutions versus pH ~ 10 for Na_2CO_3 solutions). No efforts were made to control the pH during these tests, or to examine the effect of this parameter on the generation rate because it is largely irrelevant. H_2O_2 can be generated at any pH within the range likely to be encountered in a real system; only the efficiency will be affected by pH. However, factors that determine efficiency, such as the current magnitude, bed length, and solution flow rate, can be adjusted to compensate for an unfavorable pH. The major issue becomes one of cost, which can be better assessed case by case by performing tests on actual groundwater samples. Such tests were beyond the scope of this stage of the work.

Table 6. Effect of electrolyte salt on the rate of generation of hydrogen peroxide.

Salt	Salt Conc. mM	H_2O_2 Rate $\mu\text{mol min}^{-1}$	H_2O_2 Concentration mM (ppm)	Current Efficiency %
Na_2SO_4	1.0	0.24	0.24 (8.2)	38
Na_2CO_3	1.0	0.38	0.38 (12.9)	57
$FeSO_4$	1.48	0.03	0.029 (1.0)	4

Virtually no peroxide is generated when Fe^{2+} ions are present. This is to be expected, since Fe^{2+} ions are known to catalyze decomposition of H_2O_2 to form hydroxyl radicals; we rely on this chemistry in the catalytic component of the reactor (see Background). The major objective of this test was to establish what concentration of Fe^{2+} in the electrolyte was sufficient to react with all H_2O_2 present. This is clearly less than 83 ppm for an applied current of 2 mA.

SECTION III

DEVELOPMENT AND OPTIMIZATION OF OXIDATION CATALYSTS

Initial experiments with catalysts for converting H_2O_2 to $\text{HO}\cdot$ focused on use of the classic $\text{Fe}^{2/3+}$ system (Fenton's chemistry), in the form of suspended iron oxide (FeO_x) particles. These experiments showed that the rates and efficiencies for oxidizing the model pollutants were low and strongly pH dependent. Later experiments were restricted to exploring the novel use of metallic ion (ZVI) to promote oxidation of the organics by faster and more efficient oxidation reactions.

Catalytic Efficiency of $\text{Fe}^{2/3+}$

We can stipulate several criteria for a useful catalyst to oxidize organic compounds: high cycling efficiency for decomposing H_2O_2 to $\text{HO}\cdot$, high efficiency in oxidizing aqueous organic compounds, high stability toward changes in pH and to the presence of cations and anions in groundwaters and good physical integrity to retain bulk particle size and porosity.

One feature in cycling of $\text{Fe}^{2/3+}$ for production of HO radical from H_2O_2 (Reactions 3 and 4) is the rapidity with which Fe^{2+} is regenerated from Fe^{3+} on FeO_x particles. To estimate potential catalyst cycling efficiency, we performed initial tests on two commercial iron oxides: hydrated Fe (III) oxide ($\text{FeO}(\text{OH})$) and iron (II and III) oxide (Fe_3O_4). About 10 mmoles of each iron oxide was mixed with 100 mL of water containing 80 mmoles of H_2O_2 . All hydrogen peroxide in both batches was consumed rapidly, whereas more than 95% of hydrogen peroxide remained in a control without any iron oxide, indicating that Fe^{2+} can cycle many times, a characteristic essential for long term *in situ* use. We also determined that a 350 μM hydrogen peroxide solution can be decomposed by 1.3 g (15 mmoles) of $\text{FeO}(\text{OH})$ within 10 minutes, matching the rate needed to decompose hydrogen peroxide in the electrochemical flow system, generated at about the same steady state concentration and with the same contact time (see Section II).

Oxidation of Organics with FeO_x Catalysts

Organic contaminants may be oxidized on the FeO_x catalyst surface by bound $\text{HO}\cdot$ (in the form of $\text{FeO}\cdot$ or $\text{Fe OH HO}\cdot$) or in the aqueous phase by free $\text{HO}\cdot$. To determine the rates and efficiencies of oxidation of an organic compound, we selected two model pollutant chemicals, p-cyanoacetophenone ($\text{CH}_3\text{COC}_6\text{H}_4\text{CN}$, CAP) and p-acetylbenzenesulfonate anion

($\text{CH}_3\text{COC}_6\text{H}_4\text{SO}_3^-$, ABSA) as oxidation probes and several possible FeOx catalysts from commercial sources or prepared from iron salts. CAP and ABSA are low molecular weight compounds, which have fair to good solubility ($> 0.1\%$ at 25°C) in water, low volatility, do not adsorb on glass, have high reactivity toward HO^\bullet and are easy to analyze at low concentrations.

One set of experiments was performed with $10\text{ }\mu\text{M}$ CAP (1.45 ppm) using 1.3 g (6 or 15 mmol) of either $\text{FeO}(\text{OH})$ or Fe_3O_4 in 100 mL water. Figure 1 shows the effect of adding aliquots of $180\text{ }\mu\text{M}$ (6.1 ppm) H_2O_2 (concentration in the mixture) to the mixture of iron oxide with CAP over a period of about three hours. With Fe_3O_4 , no loss of CAP was found either with or without added H_2O_2 , indicating that neither sorption of CAP to the oxide surface nor oxidation occurred.

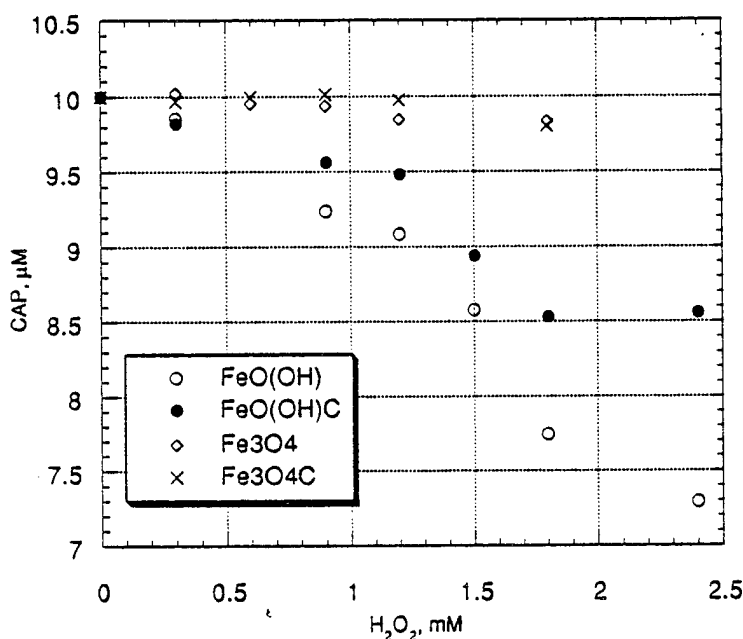


Figure 1. Loss of CAP in the presence of H_2O_2 with Fe_3O_4 with or without added H_2O_2 .

Sorption and some oxidation both occur with $\text{FeO}(\text{OH})$. The difference in loss of CAP between the experiments with and without H_2O_2 is due to oxidation of CAP on addition of more than 1.5 mM H_2O_2 ; additional evidence for oxidation comes from detection of products in high performance liquid chromatography (HPLC). However, the efficiency of oxidation with $\text{FeO}(\text{OH})$ is very low (about 0.06%), based on losses of CAP and H_2O_2 .

These two experiments illustrate the diversity of catalytic properties to be found on FeOx structures, but do not indicate whether oxidation of CAP requires prior sorption to the FeOx

particles. The earlier study of phthalic acid oxidation on precipitated FeO_x (Mill et al., 1989) indicated that prior sorption was needed.

The poor efficiency of the commercial FeO_x materials prompted us to prepare other FeO_x catalysts with more controlled properties. Two types of $\text{Fe}(\text{OH})_3$ catalysts were made, from Fe^{3+} one was filtered as a gel ($\text{FeO}(\text{OH})(\text{H}_2\text{O})_x$) (FeO (gel)) and a portion of the gel was weighed and heated to 200°C for 16 hours (Fe_2O_3). Only 12 wt % of the FeO (gel), was Fe^{3+} oxide, the remainder water.

Oxidation efficiency measurements were performed with mixtures of $10\ \mu\text{M}$ CAP, $350\ \mu\text{M}$ H_2O_2 , and $0.4\ \text{g}$ FeO (gel) or $0.2\ \text{g}$ Fe_2O_3 , stirred at 25°C and aliquots were removed at several times up to 200 minutes and analyzed for CAP and H_2O_2 . Controls without H_2O_2 showed no loss of CAP indicating that CAP was not adsorbed on the catalyst surfaces. These catalysts had oxidation efficiencies of 0.2 to 1.1%, assuming no hydrogen peroxide remains at 200 minutes. Although the oxidation efficiencies for both catalysts are somewhat higher than for $\text{FeO}(\text{OH})$ or Fe_3O_4 , both are too low for a scaled up system.

This catalyst is designated as a Fe-gel 6 catalyst for subsequent oxidation experiments with CAP and ABSA. Other oxidation experiments were designed to follow losses of both CAP and peroxide in the stirred mixtures with catalyst. Experiments with catalysts but without CAP or without peroxide allowed us to evaluate the activity of the catalysts toward peroxide or CAP alone. Peroxide was added incrementally every 10 minutes to provide initial concentrations of $180\ \mu\text{M}$ in the mixtures. All of the H_2O_2 was consumed by Fe-gel 6 after 5 minutes; with Fe-gel 7 and 10, $\approx 5\%$ peroxide remained after 5 minutes. CAP was oxidized with Fe-gel 4, but not with Fe-gel 7 or 10. A control without H_2O_2 for Fe-gel 6 indicates that CAP does not adsorb significantly on the catalyst.

Peroxide decomposes readily on the Fe-gel 7 and 10 catalysts without oxidation of CAP. Two possible explanations are that, either sorption of CAP to the surface is needed to effect oxidation and this is inhibited at higher pH, or release of surface bound HO^\bullet is needed for aqueous phase oxidation, but is prevented at high pH.

Figure 2 shows the loss of CAP, which was analyzed 10 minutes after each addition of hydrogen peroxide; CAP concentrations are plotted versus consumed H_2O_2 . Fe-gel 10 can be regenerated in a pH 4 solution to give an oxidation efficiency of 1.4%, which is better than that of Fe-gel 4. Fe-gel 4 probably can also be activated at lower pH.

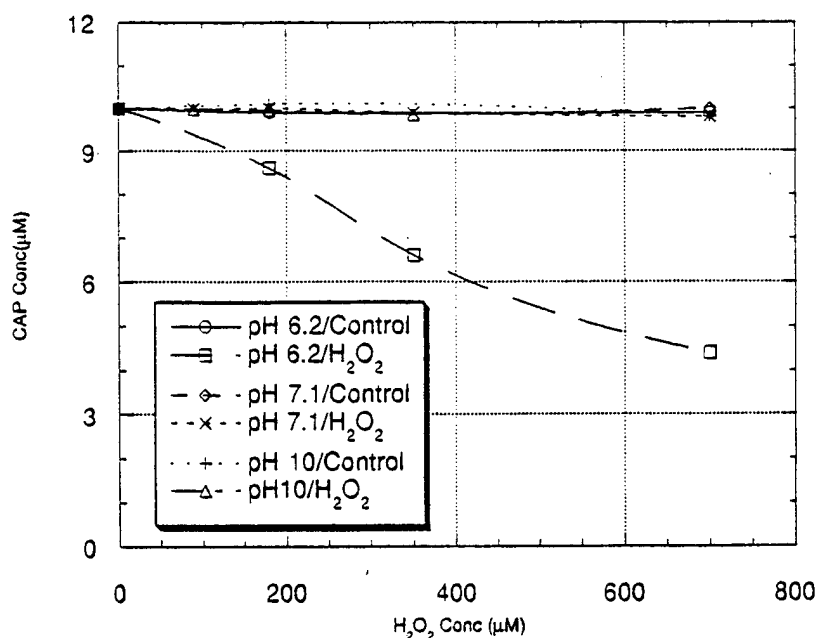


Figure 2. Measured loss of cyanoacetophenone (CAP) in the presence of H₂O₂ and Fe-gel at various pH.

Fe-gel 4,7 and 10 have very similar characteristics, except for the number of protons on the surface. However, pH is obviously a critical factor in determining oxidation efficiency. The Fe-gel 4 would be useful for groundwater at pH below 6, but for groundwater much more basic than pH 6, rates are significantly lower and adjustments would be needed to influent pH to make the oxidation rate usefully fast.

Catalysts prepared at pH 8 (see Experimental Methods) were tested with CAP (10 μM, 1.45 ppm) and incremental additions of peroxide every 10 min to restore the peroxide concentration to 180 μM (6.1 ppm). Figure 3 shows that although the pH 6 catalyst (Fe 6) is largely inactive in oxidation, Fe 5 and Fe 4 catalysts gave larger oxidation rates and efficiencies. At pH 4, we found 2.5% efficiency in oxidation. Two sequential oxidations of 10 mM ABSA, where ABSA was added after all original ABSA was oxidized, and sequential oxidation of ABSA and CAP with the same pH 4 catalyst showed that the catalyst retains its activity through several oxidation cycles (see Figures 4 and 5).

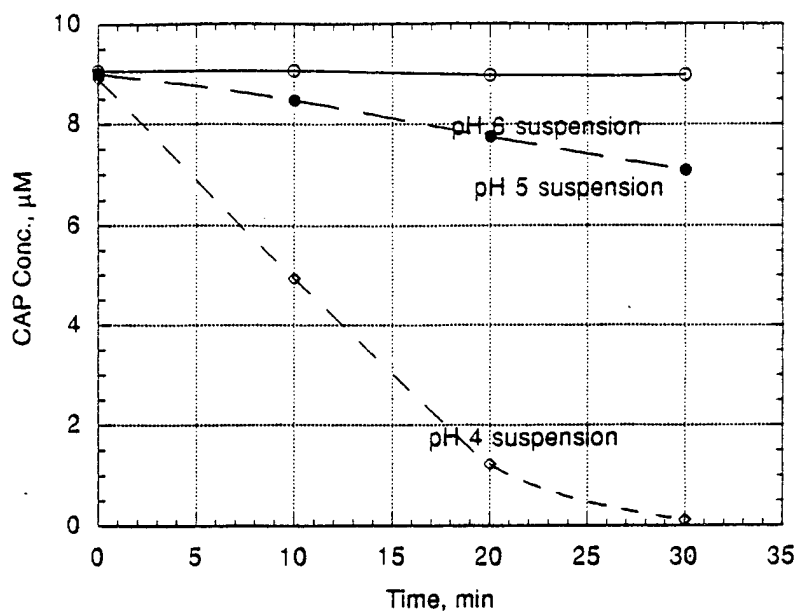


Figure 3. CAP decomposition in FeOx suspension of pH 4, 5 and 6. Each time point represents addition of H_2O_2 to give 180 mM concentration.

Two points are worth noting. First, only a small amount (10%) of ABSA sorbed to the pH 4 catalyst; second, the oxidation efficiency for the catalyst in oxidizing two sequential doses of 10 μM (2 ppm) ABSA or a sequence in which 10 μM (1.45 ppm) CAP was oxidized after oxidizing 10 μM ABSA was the same as in oxidizing 10 μM CAP initially, namely 2.5%.

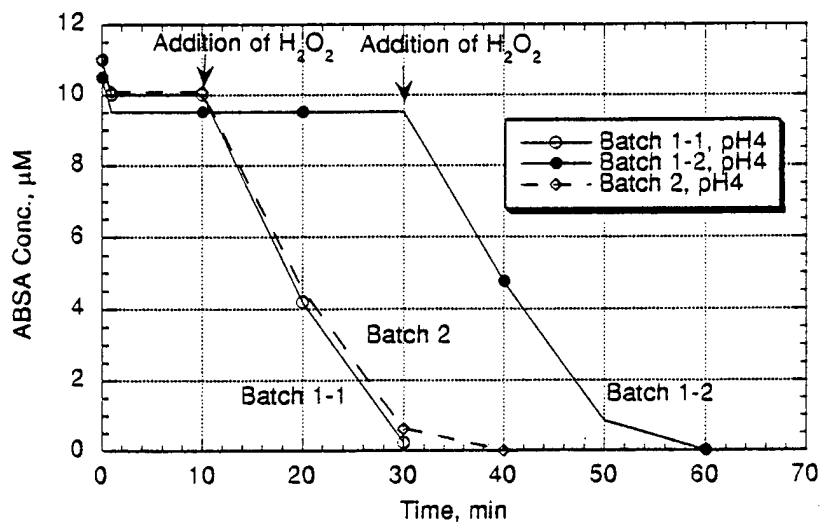


Figure 4. ABSA decomposition in pH 4 FeOx suspension. Each time point represents addition of H_2O_2 to give 180 mM concentration.

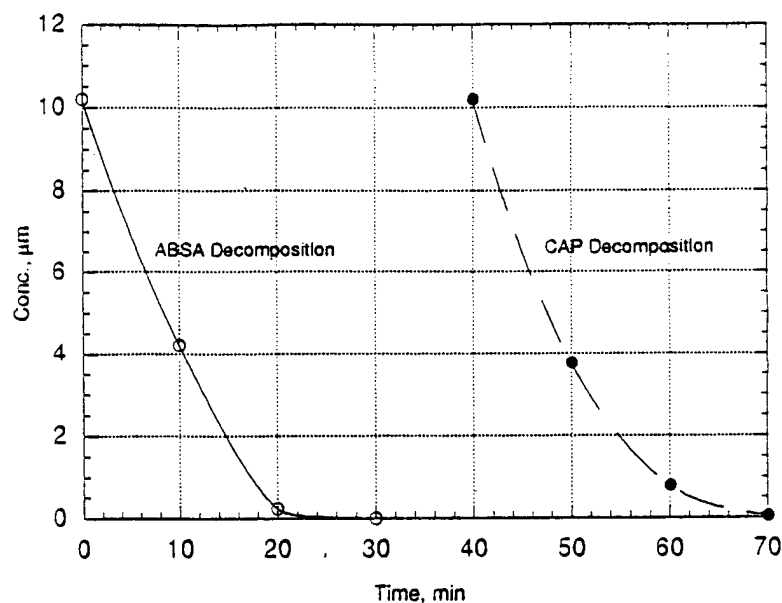


Figure 5. Sequential oxidation of ABSA and CAP with FeO_x at pH 4. Each time point represents addition of H_2O_2 to give 180 mM concentration.

We conclude from these series of experiments that we can reproducibly prepare a robust FeO_x catalyst which shows modest oxidizing efficiencies through several oxidation cycles at pH 4, but that using the FeO_x catalyst in higher pH suspensions leads to lower efficiencies.

COMPETITION KINETICS

It is important to determine the identity of the oxidizing species in these FeO_x -catalyzed reactions to know how specific or selective the oxidant is toward a variety of organic pollutants. The relative reactivities of two or more compounds in an oxidation system can be a sensitive method to identify the dominant oxidant and to compare oxidants in different systems. We used competition kinetics to determine relative reactivities of ABSA and CAP toward the oxidants present in the heterogeneous FeO_x -peroxide systems. Measurements were initially conducted at pH 2 in homogeneous solution where the reaction of Fe^{2+} in solution with peroxide is known to form $\text{HO}\cdot$ (Reaction (3), Walling, 1975), using mixtures of 10 μM each of CAP and ABSA and 33 mM Fe^{3+} (as ClO_4^- salt). Comparable oxidations in the heterogeneous system were conducted with 33 mM FeO_x suspension at pH 4. Aliquots of peroxide, adjusted to give 85 μM H_2O_2 in solution,

were added every 10 minutes to the well-stirred mixtures. At each addition time, an aliquot was removed for analysis of CAP and ABSA. The kinetic relation for competitive oxidation is:



$$k_1/k_2 = \ln([C]_t/[C]_0)/\ln([A]_t/[A]_0) \quad (9)$$

where k_1 and k_2 are rate constants for reactions (1) and (2) and $[C]$ and $[A]$ are concentrations of CAP and ABSA at time t and zero, respectively.

Figure 6 shows the loss of CAP and ABSA with time at pH 2 and Figure 7 shows a competition plot of Equation (9) for pH 2 data. The slope of the plot (k_1/k_2) is very close to 1 suggesting that CAP and ABSA have very similar reactivities toward $\text{HO}\cdot$. The different electron withdrawing substituents para to the acetyl group (sulfonate and cyano) in ABSA and CAP could lead to as much as a factor two in relative reactivities, based on the Hammett equation (Perrin, 1972); the similarity of their rates reflects the high reactivity of HO radical toward both compounds.

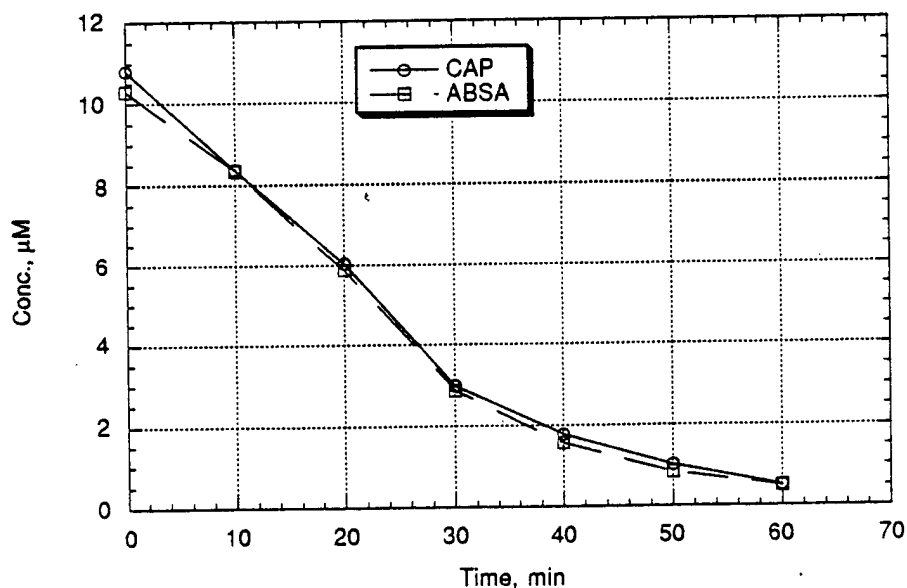


Figure 6. Competitive oxidation of CAP and ABSA in pH 2 Fe^{3+} solution with $85 \mu\text{M}$ aliquots of H_2O_2 .

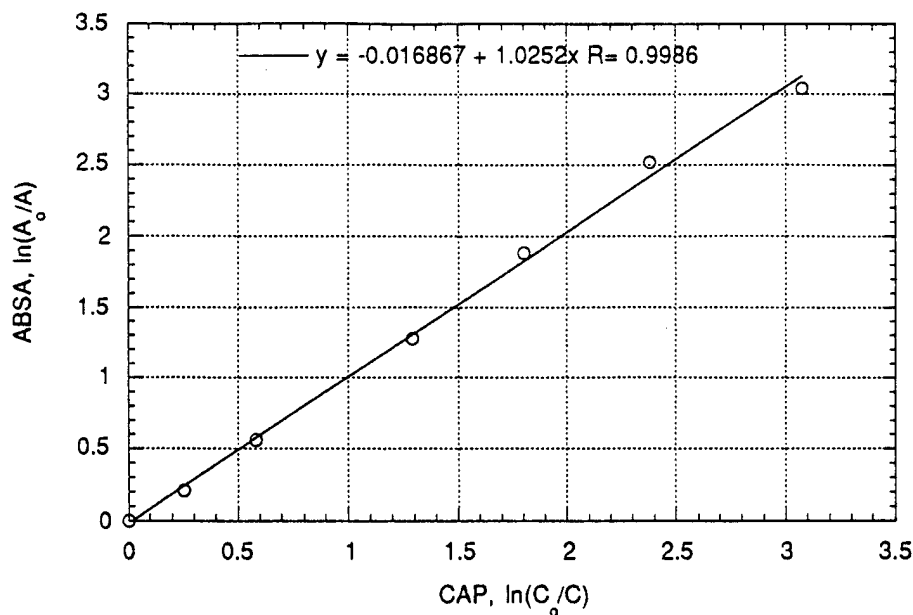


Figure 7. Competition kinetic plot of ln ABSA versus ln CAP for pH 2 oxidation.

A similar competitive oxidation of CAP and ABSA at pH 4 in the presence of FeO_x suspension gave nearly identical results to the results pH 2 in solution, strongly indicating that the same major oxidant forms in this system, either HO^\bullet or a surface-bound HO^\bullet with the same selectivity. Figures 8 and 9 show loss and competition plots for CAP and ABSA at pH 4 with a FeO_x suspension.

Low efficiencies in oxidations with FeO_x suspensions prompted us to examine briefly the use of Fe^{n+} dispersed on zeolite by ion exchange of Na-zeolite. Experiments with Fe^{3+} -exchanged zeolite gave no reaction either with H_2O_2 or with CAP. Zeolite exchanged with Fe^{2+} ion did show fairly rapid loss of 180 μM peroxide: 90 μM was lost in ~ 1 min but loss of the remaining 90 μM required 13 minutes. Reaction of 11 μM CAP with the same peroxide-zeolite suspension gave a loss of 5 μM in 1 minute, but the loss slowed to nearly zero, with 34 minutes required for oxidation of an additional 3 μM peroxide. The failure of these zeolites to sustain oxidations may be related to slow loss of Fe^{n+} back into solution, but we made no further effort to investigate these materials.

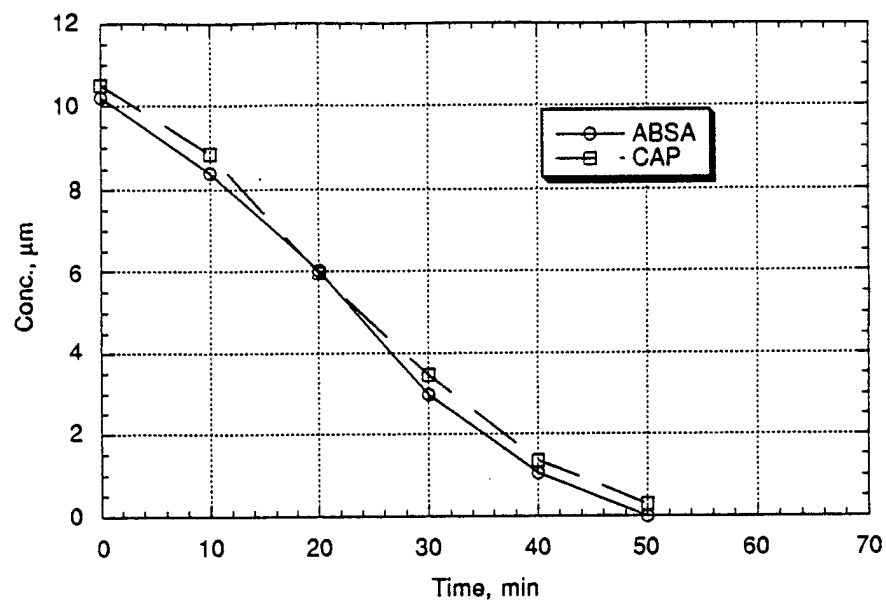


Figure 8. Competitive oxidation of CAP and ABSA in pH 4 FeO_x suspension with $85 \mu\text{M}$ aliquots of H_2O_2 .

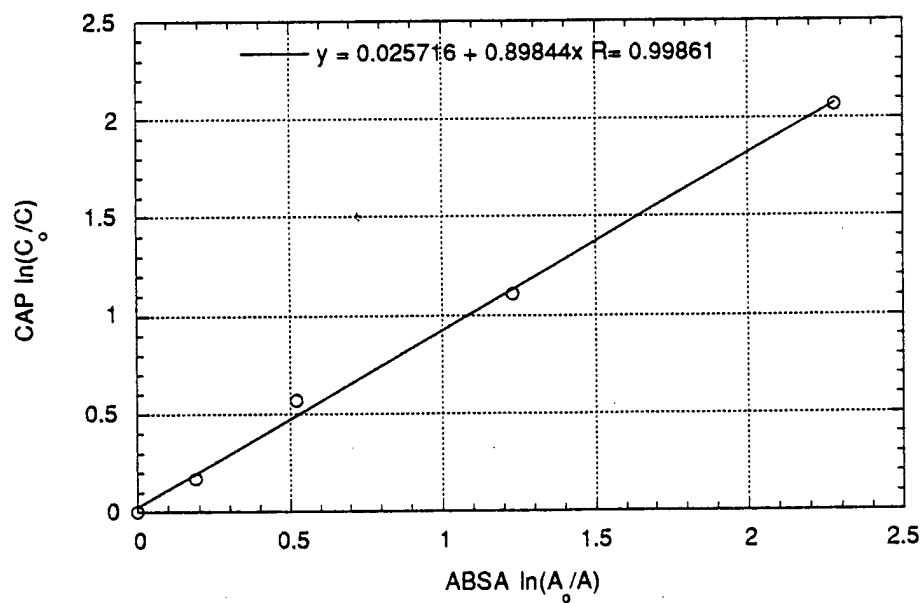
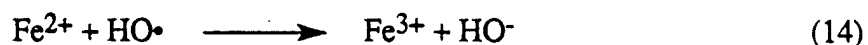
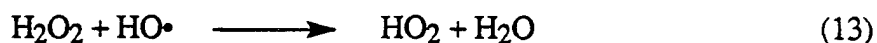
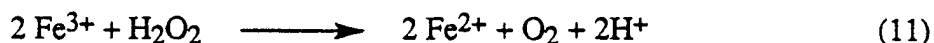
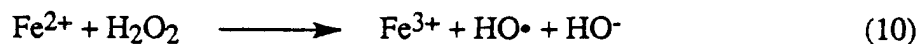


Figure 9. Competition kinetic plot of \ln CAP versus \ln ABSA for pH 4 oxidation.

A simple model for oxidation with peroxide-FeO_x mixtures may be written to include initiation of oxidation through HO radical formation from Reaction (3), oxidation of CAP or any organic (RH) by reaction with HO and competition for HO radical by H₂O₂ and Fe²⁺



From this sequence we can write the oxidation of RH as

$$d[\text{RH}]/dt = k_{12}[\text{HO}\cdot][\text{RH}] \quad (15)$$

and

$$[\text{HO}\cdot] = k_{10}[\text{Fe}^{2+}][\text{H}_2\text{O}_2] / \{k_{12}[\text{RH}] + k_{13}[\text{H}_2\text{O}_2] + k_{14}[\text{Fe}^{2+}]\} \quad (16)$$

Equation (10) shows that the rate of Reaction (12) depends on the concentrations of several competing species including RH, H₂O₂ and Fe²⁺. In this system, Fe²⁺ is probably the dominant competitor for HO radical and Equation (16) simplifies to

$$[\text{HO}\cdot] = k_{10}[\text{Fe}^{2+}][\text{H}_2\text{O}_2] / k_{14}[\text{Fe}^{2+}] \quad (17)$$

$$[\text{HO}\cdot] = k_{10}[\text{H}_2\text{O}_2] / k_{14} \quad (18)$$

which means that over a certain concentration range the rate of oxidation of RH should be independent of the amount of FeO_x present and the efficiency defined by

$$\%E = (\Delta\text{RH}/\Delta\text{H}_2\text{O}_2) \times 100 \quad (19)$$

can be rewritten

$$\%E = \{k_{12}[\text{RH}]k_{10}[\text{H}_2\text{O}_2] / k_{14}k_{10}[\text{Fe}^{2+}][\text{H}_2\text{O}_2]\} \times 100 \quad (20)$$

$$= \{k_{12}[\text{RH}] / k_{14}[\text{Fe}^{2+}]\} \times 100 \quad (21)$$

In other words efficiency is tied to the amount of FeO_x catalyst used; the more catalyst, the faster the rate, but the lower the efficiency.

Table 7 summarizes results from most of the oxidation experiments using FeO_x as a catalyst for the oxidation of CAP and/or ABSA. The fastest rates and highest efficiencies are found with Fe gel at pH 4 with 2.5%.

ZERO VALENT METAL OXIDATION PROMOTERS

The low efficiencies and low oxidation rates found for FeO_x catalysts with H_2O_2 prompted us to examine the effects of using zero valent metals reported to decompose H_2O_2 as promoters for oxidation of organics. A literature review to uncover published accounts of zero valent iron ($\text{Fe}(0)$) promoted oxidations of organics found no relevant references. Although studies to stabilize H_2O_2 against decomposition on metal surfaces are abundant and of considerable practical value, no study reported that $\text{Fe}(0)$ or other zero valent metals promoted oxidation as well (Schumb et al., 1955).

Zero valent (metallic) iron ($\text{Fe}(0)$) gives not only much higher rates of oxidation of CAP, but also much higher efficiencies than found with FeO_x -based catalysts. We also investigated oxidation rates and efficiencies using several other zero valent metals ($\text{M}(0)$). These results are discussed below as $\text{Fe}(0)$ or $\text{M}(0)$ promoted oxidations.

Fe(0) Promoted Oxidations

Comparison of the oxidation rates for CAP with $\text{Fe}(0)$ and FeO_x is found in Figure 10, where $\sim 10 \mu\text{M}$ CAP is oxidized with $\sim 200 \mu\text{M}$ H_2O_2 in the presence of 23 mM suspended $\text{Fe}(0)$ or 50 mM suspended FeO_x . The half life for oxidizing CAP with 10 μm particles of $\text{Fe}(0)$ is only 12 seconds, whereas the half life with FeO_x is 10 minutes! Figure 10 also shows that the rate is linearly related to the amount of $\text{Fe}(0)$. Figure 11 shows that roughly doubling the CAP concentration does not affect the half life for oxidation (~ 20 sec), as expected in a pseudo first-order regime with excess H_2O_2 and $\text{Fe}(0)$. Figure 12 shows that increasing the concentration of H_2O_2 from 66 to 200 μM gives half lives for CAP inversely proportional to the H_2O_2 concentration, also consistent with the pseudo-first order kinetics. Figure 13 shows that the loss rate for CAP increases by a factor of about two when the loading of $\text{Fe}(0)$ changes by a factor of two.

Table 7

OXIDATION OF CAP AND ABSA BY HYDROGEN PEROXIDE WITH DIFFERENT IRON OXIDE CATALYSTS

Expt.	pH	Compound	Init. Conc. (μ M)	Final Conc. (μ M)	H ₂ O ₂ Conc. (μ M)	Fe Oxide (Conc.) (μ M)	Rate (μ M/min)	Efficiency, (%)
1		CAP	10	10	1.8	Fe ₃ O ₄ (15)	~0	0
2		CAP	10	8.5	2.4	FeO(OH) (15)	3.5(-2)	0.06
3		CAP	10	9.3	0.35	Fe-gel (10)	3.5(-3)	0.2
4		CAP	10	6.5	0.35	Fe ₂ O ₃ (25)	1.75 (-2)	1.1
5		CAP	10	0	0.18 ^y	Fe-gel 7,10()	0	0
6		CAP	10	4	0.18 ^y	Fe-gel 4()	1.3(-1)	0.85
7		CAP	9	10	0.18 ^y	Fe 6()	0	0
8		CAP	9	6.5	0.18 ^y	Fe 5()	1.2(-1)	0.6
9		CAP	9	1	0.18 ^y	Fe 4()	4(-1)	2.5
10		ABSA ^{zz}	10	0.5	0.18 ^y	FE 4()	3(-1)	2.5
11		ABSA/CAP ^{zz}	10,10	0.0	0.18 ^y	FE(4)()	>5(-1), >5(-1)	2, 1.7

xCorrected for sorption to FeO_x catalyst.

yInitial conc. during three incremental additions.

zMinimum.

zzSequential oxidation with same catalyst of two 10 μ M ABSA or ABSA solutions and one CAP solution

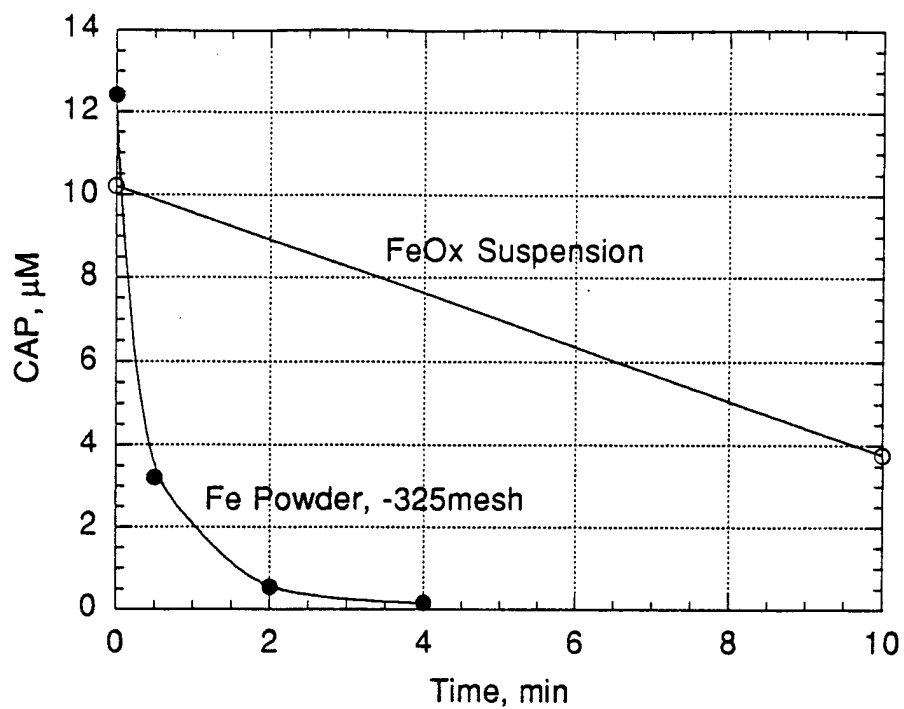


Figure 10. CAP oxidation using Fe(0) and FeO_x with H₂O₂ at pH 4.

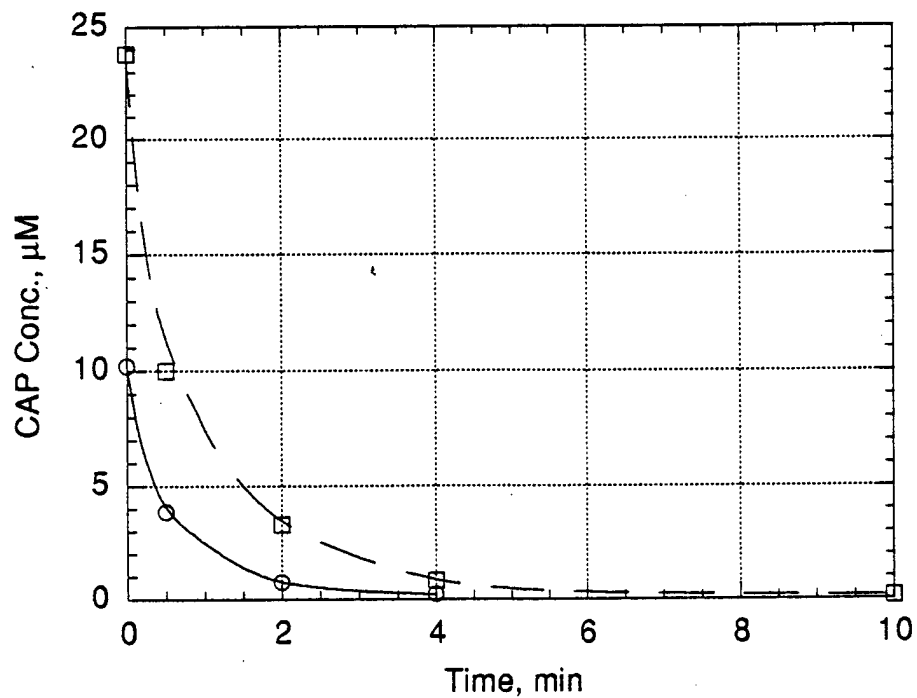


Figure 11. CAP decomposition with 10 μM Fe(0) and 200 μM H₂O₂.

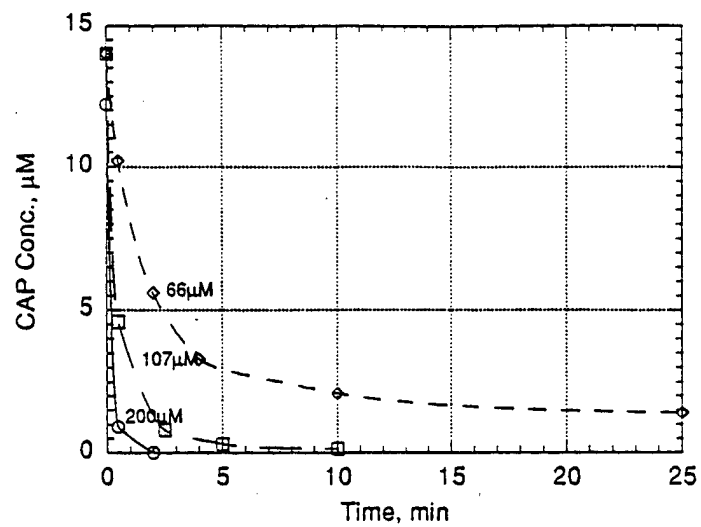


Figure 12. CAP oxidized with Fe(0) and 66-200 μM H₂O₂

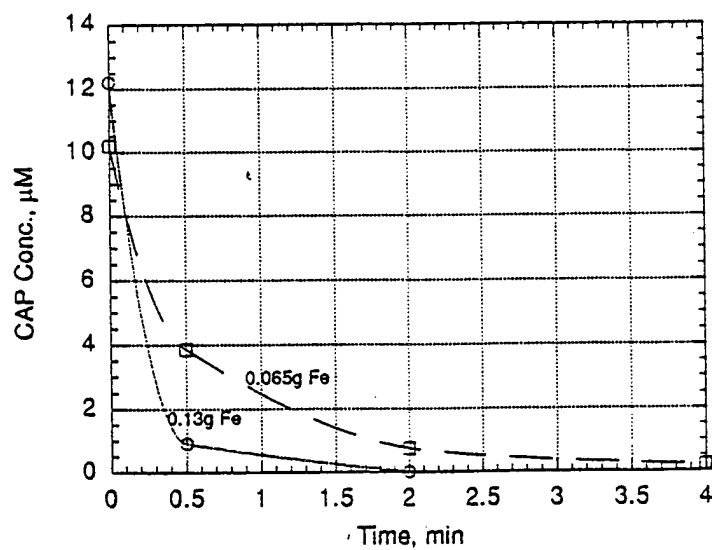


Figure 13. CAP oxidation using 0.13 g vs 0.065 g 10 μM Fe, with 0.200 mM H₂O₂.

The data of Figures 11-13 indicate that the initial rate of oxidation of CAP may be described by the relation

$$\text{Rate} = d[\text{CAP}]/dt = k_{\text{oxid}}[\text{Fe}(0)][\text{H}_2\text{O}_2][\text{CAP}] \quad (22)$$

Equation (22) says that with excess Fe(0) and H₂O₂, loss of CAP is first order, with a rate constant proportional to the concentrations of H₂O₂ and Fe(0).

One of the most important oxidation operating parameters will be pH, because of the potential sensitivity of the chemistry to Fe(0) surface conditions. Several experiments were conducted to determine pH effects in the Fe(0)-promoted oxidations and results are shown in Figure 14. The half life for 10 μM CAP is 20 sec at pH 4, 2 min at pH 5 and not measureable at pH 7 or above. Figure 14 shows plots of the data at four pH values for loss of CAP with time. The loss of HP is not as sensitive to pH; even at pH 9 some HP was lost in a time period where no loss of CAP occurred. We conclude that at higher pH values corrosion of the Fe(0) surface forms Fe(OH)₃ or FeO(OH), which either inhibit contact of CAP with the surface bound HO radicals or prevent HO from diffusing from the metal or prevent FeO(OH) surface to reach CAP in the aqueous phase.

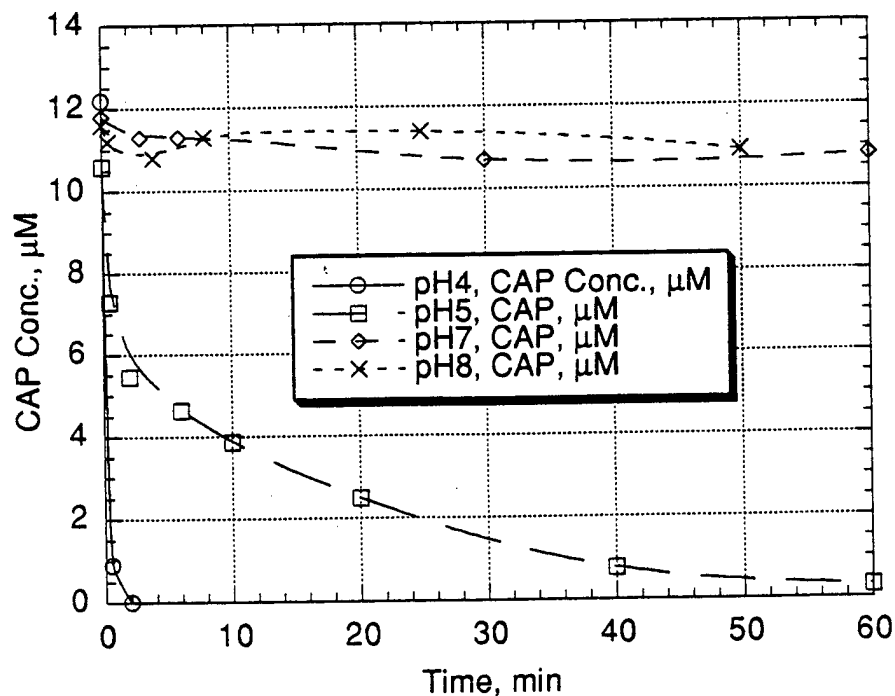


Figure 14. The effect of pH on the rate of oxidation of CAP with 22 mM 10 μM Fe(0) and 200 μM H₂O₂.

Fe(0) promoted oxidation of CAP in a flow system was evaluated using mixtures of 0.5 g/25 g Fe(0)/Ottawa sand in a 1 x 10 cm tube connected to a pump and a reservoir 10 μ M CAP and 200 μ M HP. The sand/Fe mixture disperses the Fe particles and provides better regulation of flow characteristics through the system. Slow flow rates of one mL/min or less gave high conversions of both CAP and H₂O₂, as shown in Figure 15. These slow flows are equivalent to aquifer flows of gallons/day, and are typical of many ground water aquifer flow rates (ref). Figure 15 shows that the efficiency of oxidation increases slightly as the flow rate increases from about 5% at 0.5 mL/min flow to about 10% at 10 mL/min. This pattern is consistent with the general principal that the faster rate is gained at the expense of higher efficiency, but is not dramatically affected by flow rates. Obviously the flow system was not optimized for either rate or efficiency.

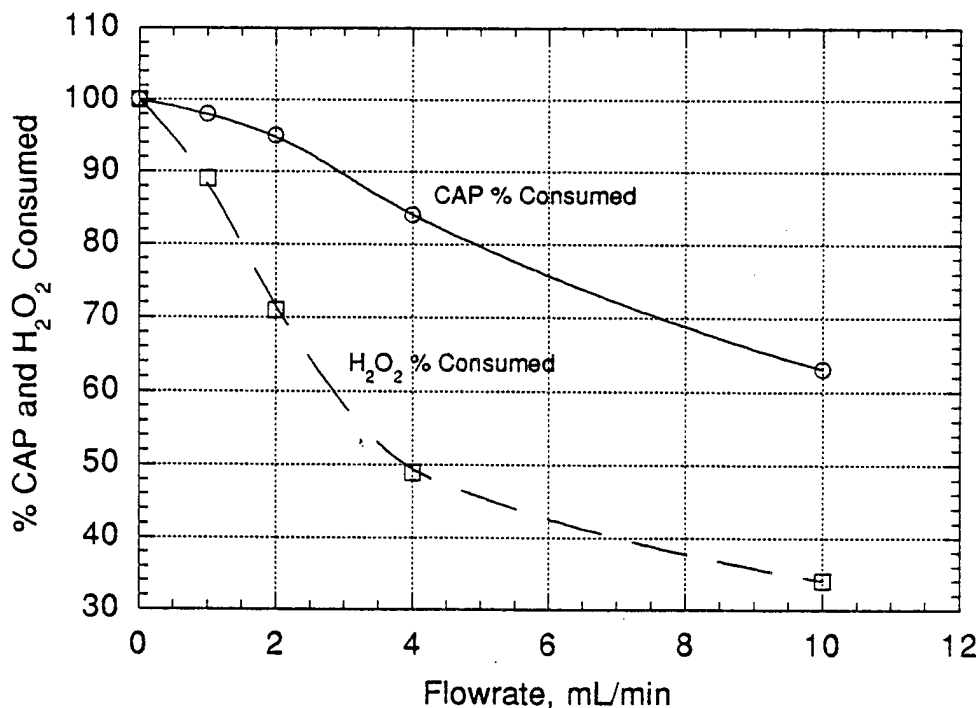


Figure 15. CAP and H₂O₂ decomposition in flow system with 0.5 g Fe/25 g sand.

M(0) PROMOTED OXIDATIONS

Many zero valent metals decompose H_2O_2 (Schumb et al., 1955), but these surface reactions do not necessarily generate $\text{HO}\cdot$ or effect the subsequent oxidation of aqueous organic compounds. Figure 16 summarizes our experiments with five different metals in addition to $\text{Fe}(0)$, all of which decompose H_2O_2 μM . Only $\text{Fe}(0)$, $\text{Cu}(0)$ and $\text{Sn}(0)$ exhibit significant promotional effects on the oxidation of CAP, but $\text{Fe}(0)$ is about one hundred times more reactive. Although different size metal particles were used in these experiments, possibly accounting for some small part of the differences in activity, the order of magnitude differences in rates of oxidation must be due largely to intrinsic differences in surface reactions with H_2O_2 and/or with CAP. Some metals ($\text{Mn}(0)$ and $\text{Cu}(0)$) decomposed H_2O_2 rapidly without concomitant oxidation of CAP, implicating sorption as a factor in the process. With other metals, such as Mg and Zn , H_2O_2 decomposition as well as oxidation are slow. The high reactivity of $\text{Fe}(0)$ coupled with its low environmental impact and low cost make it the zero valent metal of choice for the promoter in the electrochemical reactor.

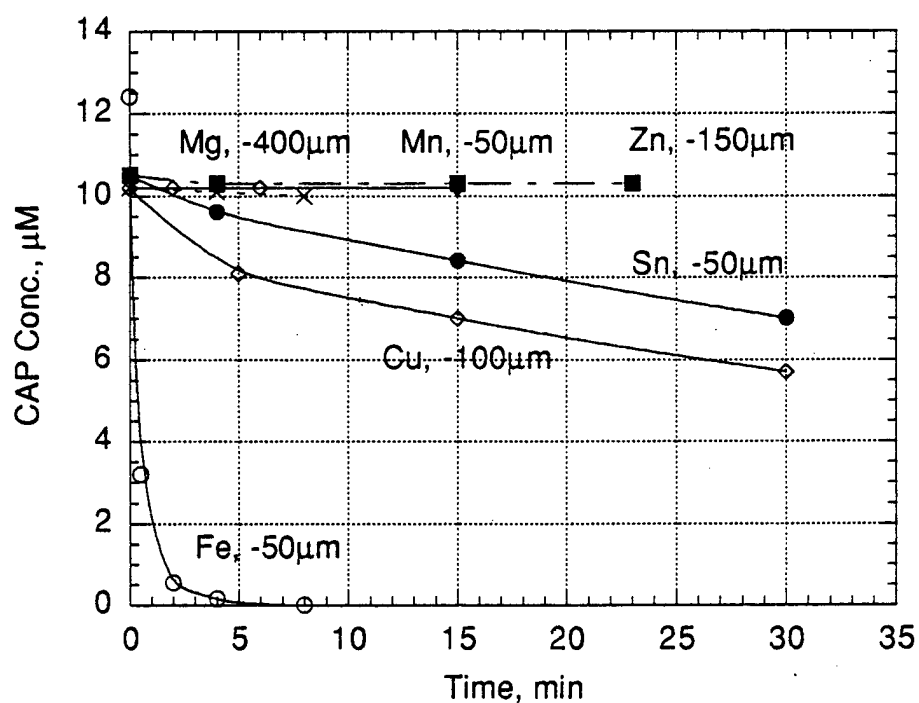


Figure 16. CAP oxidation with several metals at pH 4 with 200 μM H_2O_2 .

SECTION IV.

DISCUSSION AND CONCLUSIONS

The major conclusion that emerges from this experimental program is that the electrochemical oxidation system is feasible for use in a reactive barrier to destroy aqueous organics pollutants. We have shown that an electrochemical cell for generating H_2O_2 from water will operate over a range of natural water conditions to form useful concentrations of H_2O_2 for the subsequent oxidation process in the catalyst/promoter bed and, by using metallic iron ($\text{Fe}(0)$) as the Fenton-like promoter to convert H_2O_2 to HO^\bullet , the oxidation of organics becomes fast enough and efficient enough to be useful under field conditions. Moreover, iron particles are an economic and environmentally acceptable material for use in the barrier and their use has precedence in passive barriers undergoing field trials for treating chlorinated organics by reductive processes (Gillham and O' Hanesin, 1993).

Because the program was terminated at an early stage, we were unable to evaluate the operational features of the system using a range of natural waters or the long term stability of the system components, as originally planned. Moreover the potential for using the system in conjunction with the current passive barrier for treating chlorinated organics with metallic iron was not addressed at all.

We need to point out that although the passive iron particle barrier requires no added oxidants or reductants, its usefulness is limited to treating halogenated organics, whereas the electrochemical oxidation barrier we propose will destroy all classes of organics, including all halogenated organics, except Freon-like molecules. Thus these promising early results give us confidence that further development will lead to a useful system for treating groundwater with minimal operating costs.

The following detailed conclusions are based on results presented in Sections II and III:

- Hydrogen peroxide can be easily generated electrochemically from water at graphite felt electrodes in a once-through flow system and the concentrations of peroxide are highest when the anode is placed downstream of the cathode. Almost no peroxide is generated when the anode is placed downstream of the cathode.

- A pure DC waveform has the fastest peroxide generation rate ($0.26 \mu\text{mol min}^{-1}$ for a 0.4 mA cm^{-2} current density). However, an anodic/cathodic double pulse where both the anodic and cathodic pulses have the same duration is the most efficient at converting O_2 to H_2O_2 . The absolute duration of the pulse is not as significant as the ratio of the times of the individual pulses in determining the amount of peroxide generated.
- In general, the higher the current density the faster the H_2O_2 generation rate. However, lower current densities have higher electrical efficiencies, hence lower long-term operating costs. In terms of a field reactor, the result is a trade off between cleanup cost and cleanup time that is best determined according to the individual requirements of each case.
- FeO_x catalyze oxidation of model organics but rates and efficiencies are low and oxidation rates are much slower at $\text{pH} > 5$. at $\text{pH} 4$, FeO_x appear to be reasonably robust in effecting oxidation of several batches of organic with peroxide.
- $\text{Fe}(0)$ promotes oxidation of model organics with rapid rates and high efficiency in using peroxide.
- $\text{Fe}(0)$ promotion probably involves a $\text{H}_2\text{O}_2/\text{Fe}$ stoichiometry of 3/1 in which conversion of $\text{Fe}(0)$ to Fe^{3+} involves a sequence of rapid one-electron transfers to H_2O_2 to make 3 HO , partly accounting for the higher rates of oxidation and efficiency.
- pH effects, both with FeO_x and $\text{Fe}(0)$, may result from surface charges formed on FeO_x , resulting in lower sorption rates by either H_2O_2 or organic or both.

SECTION V. EXPERIMENTAL METHODS

ELECTROCHEMICAL EXPERIMENTS

Electrochemical Cell

Figure 17 shows the three-piece electrochemical cell used in the initial optimization study. The cell has six ports, one in the bottom for solution ingress, three in the cell body for electrical leads to the electrodes, and two in the top, one for solution egress and the other either for use as a sample port or to allow a reference electrode to be placed in the cell. The modular design of the cell allowed for the addition of a catalyst bed at either end of the cell body; however, during the electrochemical optimization study the cell was operated without a catalyst.

The cell body contained three electrodes, two counter electrodes and the working (peroxide-generating) electrode. The counter electrodes were sited one above and one below the working electrode, to enable the effect of electrode configuration on the rate of peroxide generation to be examined. The counter electrodes were made from a single piece of carbon felt, 1.1 cm thick. The working electrode was four pieces of the same felt tied together with nickel wire, giving a total electrode thickness of 4.4 cm. The cross-sectional area of both electrodes was 5.1 cm². Nickel wire was used for leads and current collectors.

The test solution was pumped from a reservoir into the cell via the inlet in the bottom piece of the cell, through the cell body which housed the peroxide-generating electrodes, and out through the outlet in the top of the cell. The cell could be operated either in recirculating mode by connecting the outlet of the cell to the inlet of the reservoir, or in one-pass mode by connecting the cell outlet to a second reservoir. Typically, experiments were performed using the one-pass mode, using a flow rate of 1 to 2 mL min⁻¹.

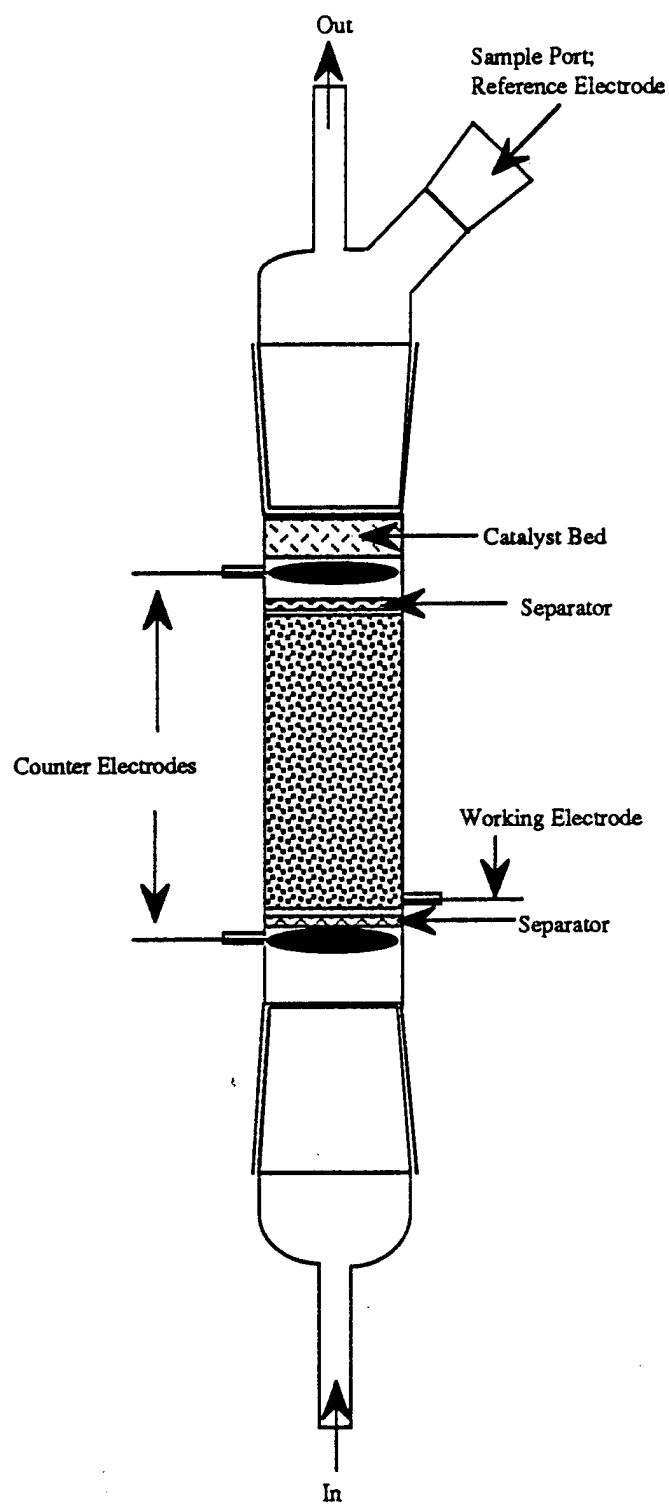
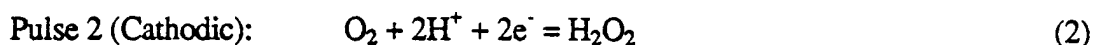
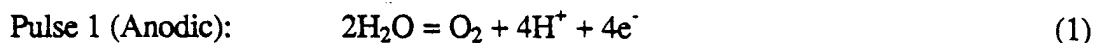


Figure 17. Electrochemical cell used to optimize hydrogen peroxide generation.

Pulse Waveform

The waveform used to generate hydrogen peroxide, shown in Figure 18, consists of an anodic pulse to generate O_2 from water, followed by a cathodic pulse to reduce the O_2 to H_2O_2 . The electrochemical reactions of interest which occur on the working electrode during these two pulses are



The initial anodic pulse has the effect of saturating the working electrode surface in O_2 and H^+ , which are the reactants required for the following H_2O_2 -generating cathodic pulse. Although the working electrode is properly considered the cell anode during the first pulse (Eq. 1) and the cathode during the second pulse (Eq. 2), for convenience it is referred to herein as the cathode, which is its function during the peroxide-generating pulse. The counter electrode is the anode.

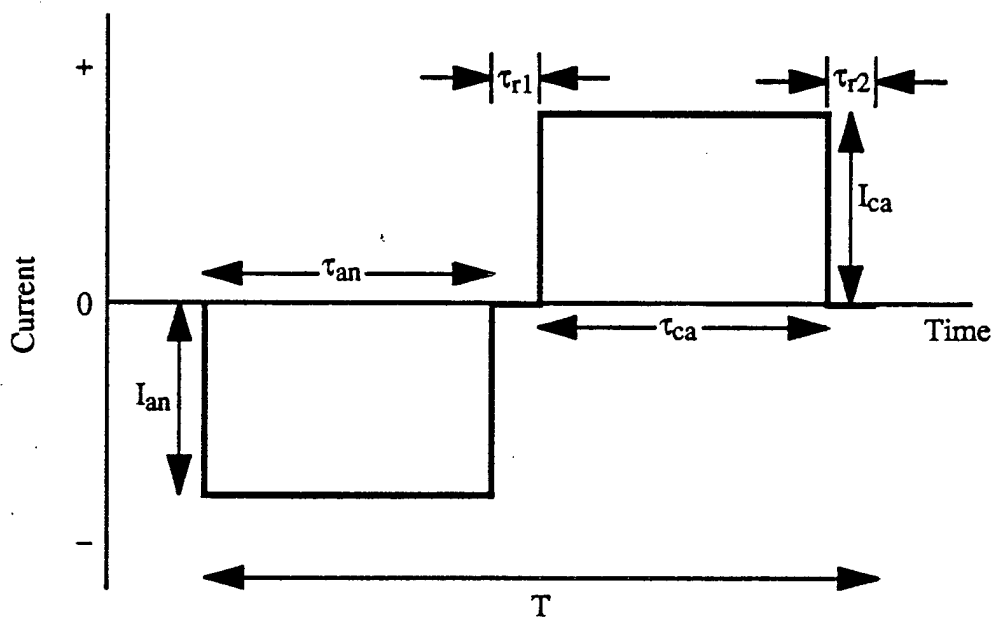


Figure 18. Pulse waveform used to generate hydrogen peroxide.

The parameters which define the shape of the waveform are the pulse width, given by the duration of the pulse, τ , and the pulse height, given by the magnitude of the pulse current, I . Thus, the anodic pulse is defined by τ_{an} and I_{an} and the cathodic pulse by τ_{ca} and I_{ca} . In addition, it may be advantageous to have a period following each pulse in which the cell is at open circuit. These periods are defined only by their duration, τ_{r1} for the open circuit period following the anodic pulse and τ_{r2} for the open circuit period following the cathodic pulse, since the current magnitude is zero for these periods. The total pulse width, T , is given by $T = \tau_{an} + \tau_{r1} + \tau_{ca} + \tau_{r2}$. These parameters are shown in Figure 18.

Table 8 summarizes the waveforms investigated in terms of these parameters. The first set of parameters, a 2 mA anodic pulse for 0.1 s followed by a 2 mA cathodic pulse for 0.4 s is the baseline experiment. This baseline was chosen based on prior results from an earlier project, and is designated Set 1. Set 2 examines the effect of using symmetrical pulse; Set 3 examines the use of a longer pulse duration at the baseline $\tau_{an}:\tau_{ca}$ ratio (0.25); and Set 4 examines a continuous DC mode of operation. The effect of current magnitude was examined using the Set 4 pulse durations, since, as described in Section 2 above, this waveform was found to be the most effective at producing H_2O_2 .

Table 8. Test values of the parameters which define the pulse waveform.

Set	Anodic Pulse		Rest time	Cathodic Pulse		Rest Time	Period
	τ_{an}/s	I_{an}/mA		τ_{ca}/s	I_{ca}/mA		
1	0.1	2	0	0.4	2	0	0.6
2	0.4	2	0	0.4	2	0	0.8
3	10	2	0	40	2	0	50
4	0	0	0	∞	2	0	∞
5	0	1	0	∞	1	0	∞
6	0	4	0	∞	4	0	∞

Test Equipment

The tests were carried out using a Princeton Applied Research Company (PARC) Model 283 Potentiostat/Galvanostat, operated in galvanostatic step-mode. This mode allows up to three current steps to be programmed. These were the anodic pulse, cathodic pulse, and a rest period

before repeating the pulse. In most experiments, the duration of the rest period was zero. The counter electrode and reference electrode terminals of the potentiostat were tied together and connected to the cell anode and the working electrode and sense terminals of the potentiostat were tied together and connected to the cell cathode.

Test solutions were pumped through the cell using a Cole-Palmer Master Flex L/S Model 7553-80 pump drive and MasterFlex L/S Model 7518-10 EasyLoad pump heads. The flow rate was 1 mL min^{-1} to 2 mL min^{-1} .

Experimental Procedures

The standard test solution of a mixture of $1 \text{ mM Na}_2\text{SO}_4$ and 1.48 mM FeSO_4 , was placed in the reservoir and the plumbing connections made between the reservoir and the cell. A second reservoir (the outlet reservoir) was connected to the cell outlet. All samples were taken from this outlet reservoir. The pump was then switched on, and after about an hour, the initial sample was taken. The outlet reservoir was again emptied, but the effluent solution was saved. The experiment was continued for another switched on. After about an hour, a second sample was taken. The outlet reservoir was again emptied, but the effluent solution was saved. The experiment was continued for another hour, after which time the final sample was taken. The effluent solutions collected during the two time periods that current was applied to the cell were mixed together and a fourth sample taken as a reality check on the two samples drawn during the test. The time between samples and the solution flow rate through the cell were such that at least one volume of the cell had passed through the system between each sample. All four samples were analyzed for peroxide using the titanium sulfate method (Satterfield and Bonnell, 1955). At the completion of the experiment the cell was rinsed with three volumes of deionized water.

CATALYST/PROMOTER EXPERIMENTS

Oxidation Test Procedures

Experiments to determine the effect of pH on oxidation efficiency used stirred mixtures of 10 uM (1.45 ppm) CAP or (2 ppm) ABSA as the model pollutants together with aliquots of $180 \text{ uM H}_2\text{O}_2$ added periodically. Aliquots were filtered with a syringe filter to remove FeOx , then analyzed for CAP or ABSA using high performance liquid chromatography (HPLC) or for hydrogen peroxide using a $\text{Ti}(\text{SO}_4)_2$ method (Satterfield and Bonnell, 1955) which gives an absorption peak at 402 nm .

Catalyst Preparation

Fe^{3+} gels were prepared from $\text{Fe}(\text{ClO}_4)_3$ by adding 1 mM NaOH to Fe^{3+} solution with constant stirring until the pH reached 9. FeO (gel) based catalysts were also prepared initially by adding aliquots of mM NaOH solution to 33 mM (1840 ppm) ferric perchlorate ($\text{Fe}(\text{ClO}_4)_3$) solution, to raise the pH to 7 or 10 and precipitate FeO (gel). The FeO (gel) suspension was either washed and used as is as a Fe-gel 7 or 10 catalyst or it was acidified to pH 4 (with HClO_4), filtered to give a pH 6 filtrate and washed with distilled water three times. The foregoing procedure for preparation of Fe-gel produces catalysts suspensions with ill-defined pH. To preparing catalysts suspensions with well-defined pH values, we adopted a simpler procedure in which $\text{Fe}(\text{ClO}_4)_3$ solution (35 mM, 1840 ppm Fe^{3+}) was basified to pH 8, stirred at pH 8 for two hours to ensure complete hydrolysis and then acidified to a new, lower pH.

Flow Oxidation Experiments

Aqueous mixtures of 180 mM H_2O_2 and 10 μM CAP were placed in a reservoir connected by Teflon tubing through a variable speed peristaltic pump (Cole- Palmer Masterflex pump) to a 4 cm dia x 8 cm long packed column containing 0.5 g 10 μm Fe(0) particles mixed in 25 g Ottawa sand. Effluent from the reactor bed was stored in a graduated cylinder and analyzed at intervals for CAP and H_2O_2 . Flow rates through the reactor appeared to be constant over time for a fixed setting of the pump, thus allowing us to calibrate the pump settings to flow rates in the reactor bed. Flow rates were initially measured from the times required to deliver fixed volumes of effluent into the cylinder at different pump settings.

Chemicals

All chemicals used for the oxidation experiments were the purest grades available from commercial sources and used without purification. Sometimes, iron particles were treated with 4 N HCl for 30 minutes and washed repeatedly with pure water before using them for some experiments. This treatment did not appear to affect the reactivity compared with untreated iron (Matheson and Tratnyek, 1994).

REFERENCES

- Cordle S. and M. Mlay, 1986. Ground Water Quality Protection. National Academy Press, Washington, D. C.
- Gillham, R. W. and S. F. O'Hannesin, 1994. Metal Enhanced Abiotic Degradation of Halogenated Aliphatics. *Ground Water* 32 : 958-967.
- Matheson, L. J. and P. G. Tratnyek, 1994. Reductive Dehalogenation of Chlorinated Methanes by Iron Metal. *Environ. Sci. Technol.* 28: 2045-2053.
- Mill, T., T. Pettit, and W. R. Haag. 1989. Oxidation Processes for Transforming Organic Compounds in Hazardous Waste Systems. In *Proceedings of the ACS Symposium on Chemical and Biochemical Detoxification of Hazardous Waste*. J. Glaser (Ed.), Lewis Publishers, Ann Arbor, MI.
- Satterfield C.N. and A. H. Bonnell, 1955. Interferences in the Titanium Sulfate Method for Hydrogen Peroxide. *Anal. Chem.* 27: 1174-1178.
- Schumb, W. C., C. N. Satterfield and R. L. Wentworth 1955. *Hydrogen Peroxide*. Reinhold Publishing Corp., New York.
- Stumm W. and J. J. Morgan, 1981. *Aquatic Chemistry*. Wiley-Interscience., Inc. New York.
- Walling, C. 1975. Fenton's Reagent Revisited. *Acct. Chem. Res.*, 8: 125-146..